VOLUME 123, NUMBER 28
JULY 18, 2001

JOURNAL OF THE AMERICAN CHEMICAL SOCIETY

Reevaluation of Stereoelectronic Contributions to the Conformational Properties of the Phosphodiester and N3′-Phosphoramidate Moieties of Nucleic Acids

Nilesh K. Banavali and Alexander D. MacKerell, Jr.*

Contribution from the Department of Pharmaceutical Sciences, School of Pharmacy, University of Maryland, Baltimore, 20 North Pine Street, Baltimore, Maryland 21201

Received February 2, 2001

Abstract: The anomeric effect in the phosphodiester backbone of nucleic acids is a stereoelectronic effect that has conventionally been linked to interactions between lone pairs on the O_{ester} atoms and $P-O_{ester}$ antibonding orbitals. The present study demonstrates that the anomeric effect in the phosphodiester backbone is significantly more complex than portrayed by this description. The presence of multiple lone pairs and antibonding orbitals around the phosphorus atom leads to additional contributions to the anomeric effect, especially involving the anionic oxygen lone pairs. On the basis of the structural changes and Natural Bond Orbital analysis it is shown that a complex balance between stereoelectronic effects involving both the ester and anionic oxygen lone pairs governs the conformational properties of the phosphodiester backbone. The N3′-phosphoramidate DNA backbone differs from the phosphodiester backbone due to the N3′−H moiety having only a single lone pair instead of the two lone pairs present on the O3′ atom substituted. The present study uses N3′-phosphoramidate as a control to understand the changes in stereoelectronic effects as a result of changes in the structure and conformation. Two previously uncharacterized properties of the N3′-phosphoramidate backbone are also observed and explained through the complex balance of the postulated electronic delocalizations. The first observation is that the N3′−H moiety in N3′-phosphoramidate is a flexible moiety that can change the orientation of its hydrogen through inversion without a significant energetic penalty in both the gas phase and the aqueous phase. The second observation is that the stabilization of the C3′-endo conformation in N3′-phosphoramidate is primarily due to aqueous solvation rather than intrinsic gas-phase effects involving the reduced electronegativity of the 3′-substituent.

Introduction

The conformational behavior of the phosphodiester backbone in nucleic acids is believed to be closely linked to the presence of stabilizing stereoelectronic effects.[1] The anomeric effect is a stereoelectronic effect related to a specific feature of the electronic structure of a molecule that results in the stabilization of one conformer over another.[2] Anomeric or gauche effects are seen for moieties with adjacent lone pair electrons and polar bonds.[2,3] Anomeric effects can exist in the phosphodiester O−P−O or phosphoramidate O−P−N3′ moieties due to delocalization of the lone pair electrons on the oxygen or nitrogen atoms into the P−O or P−N3′ antibonding (σ^*) orbitals.[4]

* To whom correspondence should be addressed: alex@outerbanks.umaryland.edu.

(1) Cramer, C. J.; Truhlar, D. G. *J. Org. Chem.* **1992**, *57*, 7034.

(2) Wolfe, S. *Acc. Chem. Res.* **1972**, *5*, 102−111.

(3) Jeffrey, G. A.; Pople, J. A.; Radom, L. *Carbohydr. Res.* **1972**, *25*, 117−123.

(4) Kirby, A. J. *The Anomeric Effect and Related Stereoelectronic Effects at Oxygen*; Springer-Verlag: New York, 1983.

10.1021/ja010295w CCC: $20.00
Published on Web 06/22/2001

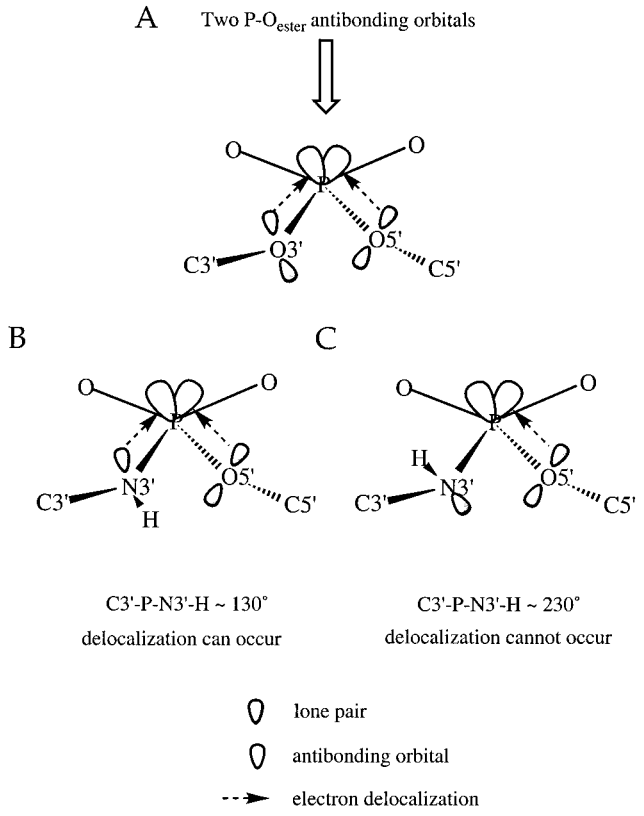

Figure 1. The conventional hypothesis of the anomeric effect responsible for the stabilization of the (A) phosphodiester and (B and C) N3′-phosphoramidate backbone in the *gg* geometries. For N3′phosphoramidate, B and C represent the two possible inversion states of the N3′H moiety. Postulated electronic delocalizations are shown by arrows. The P−O$_{ester}$ antibonding orbitals refer to the P−O3′ or P−O5′ antibonding orbitals. A general rule of thumb for the orientation of the antibonding orbital acceptor lobes is that they are located in the opposite direction of the bond. It should be noted that in this and other figures, only the lobe of the antibonding orbital that is spatially oriented to be involved to the greatest extent in the delocalizations has been shown for the sake of clarity.

The conventional view of the anomeric effect in the phosphodiester backbone is illustrated in Figure 1A. The *gg* conformation is stabilized through O$_{ester}$ lone pair electron interactions with spatially proximal P−O$_{ester}$ antibonding orbitals.[5] While this explanation makes intuitive sense, it omits possible contributions from the O$_{anionic}$ lone pairs and the P−O$_{anionic}$ antibonding orbitals. It may be argued that rotation around the P−O$_{ester}$ bonds only changes the orientation of the O$_{ester}$ lone pairs and not the O$_{anionic}$ lone pairs such that the O$_{anionic}$ lone pairs need not be considered. This argument is, however, untested and also ignores the presence of P−O$_{anionic}$ antibonding orbitals into which delocalizations from the O$_{ester}$ lone pairs can occur.

The N3′-phosphoramidate moiety differs from the phosphodiester moiety of oligonucleotides by a N3′−H replacing the O3′ atom,[6] leading to one less delocalizable lone pair of electrons. This omission of one lone pair makes the phosphoramidate moiety a good control system for studying the anomeric effect.[5,7] The 3′-nitrogen in 3′-phosphoramidate is assumed to be tetrahedral, such that the hydrogen attached to the nitrogen has two possible minimum energy positions associated with inversion about the nitrogen.[8] During this inversion the hydrogen and the lone pair exchange their positions through rehybridization. This reorientation of the N3′ lone pair leads to changes in its delocalization to the P−O5′ antibonding orbital, as shown schematically in Figure 1, parts B and C. On the basis of the presence or absence of the delocalization event shown in Figure 1, it may be anticipated that significant energetic differences would occur between the two N3′−H inversion states.

The hydrogen in the N3′−H moiety of 3′-phosphoramidate DNA is considered to be important for its duplex-forming properties based on the observation that replacing this hydrogen with the bulkier −CH$_3$ group leads to a loss of duplex-forming ability.[6] Both the NMR and X-ray crystal structures predict the orientation of the hydrogen to be such that the C3′−P−N3′−H improper dihedral is ∼130°. In the crystal structure, the N3′−H orientation is predicted on the basis of the presence of a putative hydrogen bond between the N3′−H and a Cl$^-$ ion.[9] In the NMR structure determination, no peak was obtained for the hydrogen attached to the 3′-nitrogen in aqueous solution leading to the structure determination being carried out separately for both N3′−H orientations. This led to two separate model structures with the model structure having the lower energy based on AMBER[10] force field energy minimization calculations observed to be consistent with the predictions of the crystal structure.[11] The possibility that the N3′−H group is not a rigid moiety but can exist in an equilibrium between the two possible positions has been postulated elsewhere,[11] but has not been investigated.

N3′-Phosphoramidate-substituted DNA analogues primarily populate both the C3′-endo sugar conformation and the A-form in aqueous solution[11,12] and in a crystal environment.[9] Stabilization of the C3′-endo sugar pucker in these analogues is postulated to be due to the decreased electronegativity of the N3′ atom as compared to the O3′ atom leading to a weakening of the O4′−C4′−C3′−O3′ gauche effect postulated to favor the C2′-endo conformation.[13] Evidence for this relationship between the electronegativity of the 3′-substituent on the sugar and its pucker conformation is obtained from aqueous solution studies of thymine nucleoside analogues having 3′-substituents with different electronegativity characteristics.[13,14] However, the aqueous environment present in those studies makes it difficult to judge whether the dependence on 3′-substituent electronegativity is due to intrinsic effects observable in the gas phase or due to solvation effects.

In the present study, we test the conventional view of the anomeric effect by using QM calculations on representative model compounds. Comparisons of geometries, conformational properties, NBO delocalization energies and charges, and relative energies of the minimum energy conformations for the model compounds are used to characterize the complexity of stereoelectronic effects prevalent in the phosphodiester and N3′-phosphoramidate moieties. The minimum energy orientation and

(5) Saenger, W. *Principles of Nucleic Acid Structure*; Springer-Verlag: New York, 1984.
(6) Gryaznov, S. M.; Lloyd, D. H.; Chen, J.-K.; Schultz, R. G.; DeDionisio, L. A.; Ratmeyer, L.; Wilson, W. D. *Proc. Natl. Acad. Sci. U.S.A.* **1995**, *92*, 5798−5802.
(7) Eschenmoser, A.; Dobler, M. *Helv. Chim. Acta* **1992**, *75*, 218−259.
(8) Cieplak, P.; Cheatham, T. E., III; Kollman, P. A. *J. Am. Chem. Soc.* **1997**, *119*, 6722−6730.
(9) Tereshko, V.; Gryaznov, S.; Egli, M. *J. Am. Chem. Soc.* **1998**, *120*, 269−283.
(10) Weiner, P. K.; Singh, U. C.; Kollman, P. A.; Caldwell, J.; Case, D. A. *AMBER*, 3.0 ed.; University of California: San Francisco, 1986.
(11) Ding, D.; Gryaznov, S. M.; Wilson, W. D. *Biochemistry* **1998**, *37*, 12082−12093.
(12) Ding, D.; Gryaznov, S. M.; Lloyd, D. H.; Chandrasekaran, S.; Yao, S.; Ratmeyer, L.; Pan, Y.; Wilson, W. D. *Nucleic Acids Res.* **1996**, *24*, 354−360.
(13) Thibadeau, C.; Plavec, J.; Garg, N.; Papchikin, A.; Chattopadhyaya, J. *J. Am. Chem. Soc.* **1994**, *116*, 4038−4043.
(14) Plavec, J.; Tong, W.; Chattopadhyaya, J. *J. Am. Chem. Soc.* **1993**, *115*, 9734−9746.

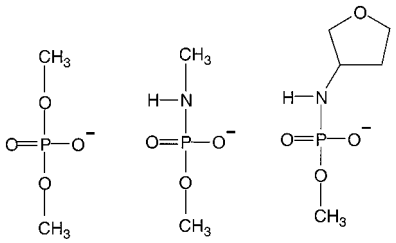

1 **2** **3**

Figure 2. Model compounds used to study the properties of the phosphodiester and N3′-phosphoramidate moieties.

conformational flexibility of the N3′−H group is also studied and the stereoelectronic delocalizations contributing to this behavior are postulated. The effects of C2′-endo (representative of B-DNA) and C3′-endo (representative of A-DNA) deoxyribose sugar conformations on the behavior of the N3′−H moiety are also studied explicitly. Solvation effects on the inversion surface are studied using reaction field calculations.[1] Differences in the solvation phase energies for the C2′-endo and C3′-endo sugar pucker surfaces are used to propose a link between aqueous solvation and the C3′-endo sugar pucker preference observed in N3′-phosphoramidate DNA.

Methods

The model compounds used for the ab initio calculations are shown in Figure 2. Ab initio calculations were performed using Gaussian 94 and Gaussian 98[15] with the MP2 level of theory to treat electron correlation. The 6-31+G* basis set was used for all calculations. The C2′-endo and C3′-endo conformations for **3** were obtained by individually constraining the endocyclic dihedrals, C3′−C4′−O4′−C1′ and C1′−C2′−C3′−C4′, respectively, to 0.0°.[16] Unconstrained geometry optimizations were performed on **1** and **2** in conformations corresponding to the *gg*, *gt*, and *tt* minima. The dihedrals describing the *g* and *t* conformations are the C3′−O3′(N3′)−P−O5′ and O3′(N3′)−P−O5′−C5′ torsions (Figure 1). The chirality imposed by the tetrahedral nitrogen atom in the phosphoramidate backbone allows for two possible orientations of the hydrogen on the nitrogen. In **2** and **3**, the inversion from one orientation to the other was studied by gradually varying the improper dihedral C3′−P−N3′−H from 100° to 250° in 15° increments. Energy barriers on the inversion surfaces were verified as transition states via vibrational analysis. The minimum energy conformations were obtained by optimization in the absence of the improper dihedral constraint. Aqueous solvation contributions were analyzed by calculating single-point energies for the minimum energy conformations using the isodensity surface polarized continuum model (IPCM)[17] with a dielectric constant of 78.36 and isodensity of 0.0004 au. Even with the assumption of an isotropic continuum solvent environment, previous studies have shown that single-point energy calculations on gas-phase optimized geometries can be a reasonable approximation to the solvation phase energy surface.[18,19] Specific electronic delocalization energies in the gas phase were obtained by using the perturbative NBO analysis[20] implemented in the NBO 3.1 program[21] on selected gas-phase minimum energy optimized conformations.

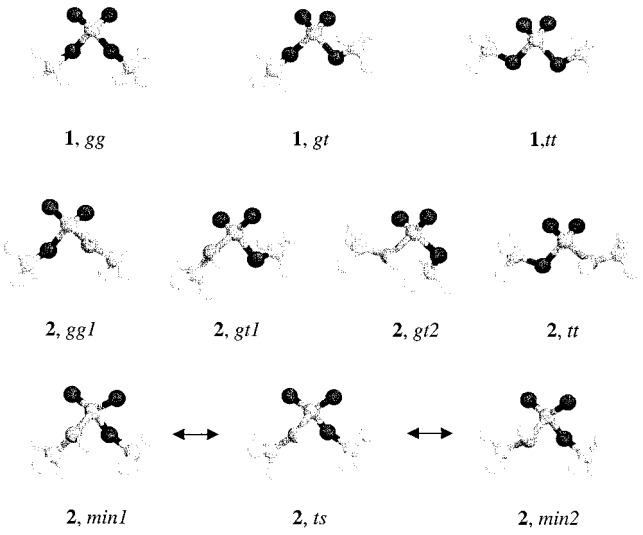

Figure 3. Selected structures for compounds **1** and **2**, including the inversion transition of the N3′-H moiety for the *gg2* geometry in **2**. For the transition *min1*, first minimum, C3′−P−N3′−H improper ∼ 130°; for *ts*, transition state, C3′−P−N3′−H improper ∼ 190°; and for *min2*, second minimum, C3′−P−N3′−H improper ∼ 230°.

Results and Discussion

1. The Anomeric Effect. a. Minimum Energy Conformations. Conformational properties of both the phosphodiester and phosphoramidate moieties are believed to be strongly influenced by the anomeric effect.[5,9] The orientation of the lone pairs on the O_{ester} atoms changes upon rotation around the P−O_{ester} bonds of the phosphodiester moiety.[5] The change in their orientations is expected to affect the nature of the stereoelectronic effects stabilizing the moiety, resulting in a change in relative energy. The geometries corresponding to the *gg*, *gt*, and *tt* energy minima have been optimized for **1** and **2** (Figure 3 and Table 1). The relative energies of these geometries in the gas phase (Table 1) indicate that the *gg* geometry is the most stable in both **1** and **2**, confirming previous observations for the phosphodiester moiety.[22−28] Due to the asymmetry introduced by the presence of the 3′ nitrogen in the N3′-phosphoramidate moiety (Figure 1), there are two distinct *gt* geometries to be considered for the phosphoramidate moiety, represented as *gt1* and *gt2*. The two possible *gg* geometries, named *gg1* and *gg2*,

(15) Frisch, M. J.; Trucks, G. W.; Schlegel, H. B.; Scuseria, G. E.; Robb, M. A.; Cheeseman, J. R.; Zakrzewski, V. G.; Montgomery, J. A., Jr.; Stratmann, R. E.; Burant, J. C.; Dapprich, S.; Millam, J. M.; Daniels, A. D.; Kudin, K. N.; Strain, M. C.; Farkas, O.; Tomasi, J.; Barone, V.; Cossi, M.; Cammi, R.; Mennucci, B.; Pomelli, C.; Adamo, C.; Clifford, S.; Ochterski, J.; Petersson, G. A.; Ayala, P. Y.; Cui, Q.; Morokuma, K.; Malick, D. K.; Rabuck, A. D.; Raghavachari, K.; Foresman, J. B.; Cioslowski, J.; Ortiz, J. V.; Stefanov, B. B.; Liu, G.; Liashenko, A.; Piskorz, P.; Komaromi, I.; Gomperts, R.; Martin, R. L.; Fox, D. J.; Keith, T.; Al-Laham, M. A.; Peng, C. Y.; Nanayakkara, A.; Gonzalez, C.; Challacombe, M.; Gill, P. M. W.; Johnson, B.; Chen, W.; Wong, M. W.; Andres, J. L.; Gonzalez, C.; Head-Gordon, M.; Replogle, E. S.; Pople, J. A. *Gaussian 98*, Revision A, 6th ed.; Gaussian Inc.: Pittsburgh, PA, 1998.

(16) Foloppe, N.; MacKerell, A. D., Jr. *J. Phys. Chem. B* **1999**, *103*, 10955−10964.

(17) Foresman, J. B.; Keith, T. A.; Wiberg, K. B.; Snoonian, J.; Frisch, M. J. *J. Phys. Chem.* **1996**, *100*, 16098−16104.

(18) Pitarch, J.; Moliner, V.; Pascual-Ahuir, J.-L.; Silla, E.; Tunon, I. *J. Phys. Chem.* **1996**, *100*, 9955−9959.

(19) Shapley, W. A.; Bacskay, G. B.; Warr, G. G. *J. Phys. Chem. B* **1998**, *102*, 1938−1944.

(20) Foster, J. P.; Weinhold, F. *J. Am. Chem. Soc.* **1980**, *102*, 7211−7218.

(21) Glendening, E. D.; Reed, A. E.; Carpenter, J. E.; Weinhold, F. *NBO*, 3.0 ed.: Madison.

(22) MacKerell, A. D., Jr.; Wiórkiewicz-Kuczera, J.; Karplus, M. *J. Am. Chem. Soc.* **1995**, *117*, 11946−11975.

(23) Florián, J.; Baumruk, V.; Strajbl, M.; Bednárová, L.; Stepánek, J. *J. Phys. Chem.* **1996**, *100*, 1559−1568.

(24) Liang, C.; Ewig, C. S.; Stouch, T. R.; Hagler, A. T. *J. Am. Chem. Soc.* **1994**, *116*, 3904−3911.

(25) Cornell, W. D.; Cieplak, P.; Bayly, C. I.; Gould, I. R.; Merz, K. M., Jr.; Ferguson, D. M.; Spellmeyer, D. C.; Fox, T.; Caldwell, J. W.; Kollman, P. A. *J. Am. Chem. Soc.* **1995**, *117*, 5179−5197.

(26) Gorenstein, D. G.; Kar, D. *J. Am. Chem. Soc.* **1977**, *99*, 672−677.

(27) Perahia, D.; Pullman, B.; Saran, A. *Biochim. Biophys. Acta* **1974**, *340*, 299−313.

(28) Sasisekharan, V.; Lakshminarayanan, A. V. *Biopolymers* **1969**, *8*, 505−514.

Table 1. Relative Energies of **1** and **2** in Various Minimum Energy Geometries in the Gas Phase and Aqueous Phase[a]

conformation of **1**	gas phase energy	aqueous phase energy	O5′−P−O3′−C dihedral	N3′−P−O5′−C dihedral
gg	0.00	0.00	69.8	69.8
gt	1.37	1.02	69.3	196.2
tt	3.34	1.43	179.7	180.8

conformation of **2**	gas phase energy	aqueous phase energy	O5′-P−N3′−C dihedral	N3′−P−O5′−C dihedral
gg1	0.00	0.99	82.3	70.2
gg2	0.00	0.99	277.8	289.8
gt1	0.43	0.00	300.7	169.3
gt2	0.91	1.47	209.2	70.1
tt	2.93	1.64	144.0	164.1

[a] Energies in kcal/mol, dihedral angles in deg. Dihedral angles associated with the minima are shown in columns 4 and 5. For **2** the reported structures correspond to the lowest energy N3′-H inversion states.

Table 2. Bond Lengths for Various MP2/6-31+G(d) Optimized Geometries of **1** and **2**[a]

conformation **1**	bond lengths			
	P−O3′	P−O5′	P−O1	P−O2
gg	1.684	1.684	1.501	1.501
gt	1.667	1.692	1.509	1.500
tt	1.634	1.634	1.477	1.477

conformation **2**	bond lengths			
	P−N3′	P−O5′	P−O1	P−O2
gg1	1.740	1.681	1.513	1.518
gg2	1.740	1.681	1.518	1.513
gt1	1.713	1.707	1.516	1.517
gt2	1.746	1.679	1.515	1.518
tt	1.726	1.688	1.517	1.524

[a] Bond lengths in Å.

are also considered for the phosphoramidate moiety to establish their energetic equivalence. In the phosphodiester moiety (**1**), the *gt* geometry is 1.4 kcal/mol higher in energy than the *gg* geometry (Table 1). In the phosphoramidate moiety (**2**), the gas phase *gt1* geometry is more stable than the *gt2* geometry by 0.5 kcal/mol and only 0.4 kcal/mol higher in energy than the *gg1* or *gg2* geometries. This observation suggests the presence of a special stabilization of the *gt1* geometry of the phosphoramidate moiety in the gas phase.

It has been suggested that environmental effects play a more important role in the conformational flexibility of **1** than stereoelectronic effects.[29] The presence of water is known to affect the energetics of the phosphodiester moiety.[30] To characterize the effect of aqueous solvation, the relative energies of the different geometries were studied in the aqueous phase represented by the IPCM reaction field model. As expected, the relative energies of the different geometries change upon inclusion of the aqueous environment. Overall, the energy differences between the various conformers decrease upon going to the aqueous phase. In **1**, the *gg* geometry remains the most stable geometry and the *gt* geometry is seen to be more stable than the *tt* geometry. In **2**, the *gt1* geometry becomes the most stable geometry followed by the *gg1* and *gg2* geometries, while the *tt* geometry remains the highest energy conformation (Table 1). These observations are consistent with previous studies on dimethyl phosphate (**1**) which show the *gg* geometry to have the lowest energy and the energy differences between the different conformations to be reduced in the aqueous phase as compared to the gas phase.[30,31]

b. Structural Evidence for the Anomeric Effect. The presence of an anomeric effect can be detected by bond length and angle changes in response to the change in the dihedral angles responsible for converting one isomer into another.[32] Dihedral angle changes alter donation of electrons from lone pairs into antibonding orbitals. The donor bond is the bond containing the atom having the lone pair and the central phosphorus atom, and the acceptor bond has the antibonding orbital accepting the lone pair. In the presence of an anomeric effect, the donor bond shortens because it has increased π character, the acceptor bond lengthens because the antibonding orbital gets populated, and the angle between the two bonds widens due to orbital rehybridization at the central atom.[33]

Changes in the bond lengths and bond angles in **1** and **2** for the different minimum energy geometries are shown in Tables 2 and 3. Inspection of Tables 2 and 3 shows variations in the P−O1 and P−O2 bond lengths and in the O1−P−X and O2−P−X angles as a function of conformation. In addition to changes in the $P-O_{ester}$ or P−N bonds there are also changes in the $P-O_{anionic}$ bond lengths in response to the geometry. This is evidence that changes occur in the delocalizations for the $O_{anionic}$ lone pairs and $P-O_{anionic}$ bonds as a result of $P-O_{ester}$ and P−N bond rotations. The change in bond distances and angles can be correlated to the presence of specific delocalizations. For example, the geometric consequence of delocalizations is seen clearly for the *gt1* geometry of **2** where there is shortening of the P−N3′ bond indicating that the N3′ lone pair is being delocalized and an enlargement of the P−O5′ bond indicating that the P−O5′ antibonding orbital is accepting a lone pair (Table 2). A similar effect is observed in the *gt* geometry of **1**, where the P−O3′ bond shortens and the P−O5′ bond lengthens in comparison to the *gg* geometry (Table 2). For the *gt* geometry of **1**, P−O anionic bond lengths also show variations. For example, the P−O1 bond lengthens and the P−O2 bond shortens as compared to the *gg* geometry (Table 2). It must be noted, however, that the presence of multiple delocalizations has to be considered to explain all the geometric changes (see next section).

c. NBO Analysis of the Anomeric Effect. In addition to the structural changes mentioned above, several studies have characterized the anomeric effect in various chemical moieties[1,32−35] by studying delocalization energies quantitatively using Natural Bond Orbital (NBO) analysis.[36] These delocalization energies are the stabilizing energies calculated by second-order perturbation theory analysis relative to an ideal Lewis structure.[36] It has been stipulated that due to the perturbative nature of this analysis the absolute magnitudes of the delocalization energies calculated may be less meaningful than their relative magnitudes.[34] It should be noted that the anionic nature of the phosphodiester and phosphoramidate moieties and the presence of multiple lone pairs of electrons complicates the study of intrinsic stereoelectronic effects, especially since solvation effects, which are not included in the NBO analysis, are not negligible for charged systems.[33]

(29) Alber, F.; Folkers, G.; Carloni, P. *J. Phys. Chem. B* **1999**, *103*, 6121−6126.
(30) MacKerell, A. D., Jr. *J. Chim. Phys.* **1997**, *94*, 1436−1447.
(31) Florián, J.; Strajbl, M.; Warshel, A. *J. Am. Chem. Soc.* **1998**, *120*, 7959−7966.
(32) Thatcher, G. R. J. *The Anomeric Effect and Associated Stereoelectronic Effects*; Comstock, M. J., Ed.; American Chemical Society: Washington, DC, 1993.
(33) Cramer, C. J. *J. Mol. Struct. Theochem* **1996**, *370*, 135−146.
(34) Cramer, C. J.; Truhlar, D. G. *Carbohydr. Res.* **1997**, *298*, 1−14.
(35) Cramer, C. J. *Theor Chem. Acc.* **2000**, *103*, 308−310.
(36) Reed, A. E.; Weinhold, F. *J. Chem. Phys.* **1983**, *78*, 4066−4073.

Table 3. Bond Angles for Various MP2/6-31+G(d) Optimized Geometries of **1** and **2**[a]

conformation	bond angles					
1	O5′−P−O3′	O1−P−O3′	O2−P−O3′	O1−P−O2	O1−P−O5′	O2−P−O5′
gg	98.3	108.9	105.6	126.0	105.6	108.9
gt	95.3	109.9	107.1	123.9	107.1	109.8
tt	94.3	109.6	109.6	120.9	109.6	109.6
conformation	bond angles					
2	O5′−P−N3′	O1−P−N3′	O2−P−N3′	O1−P−O2	O1−P−O5′	O2−P−O5′
gg1	99.0	110.7	105.3	124.7	104.9	109.4
gg2	99.0	105.3	110.7	124.7	109.4	104.9
gt1	98.0	108.0	109.2	123.8	108.1	106.7
gt2	99.1	110.1	106.1	124.6	105.1	109.0
tt	96.6	107.8	110.9	122.3	109.8	106.5

[a] Bond angles in degrees.

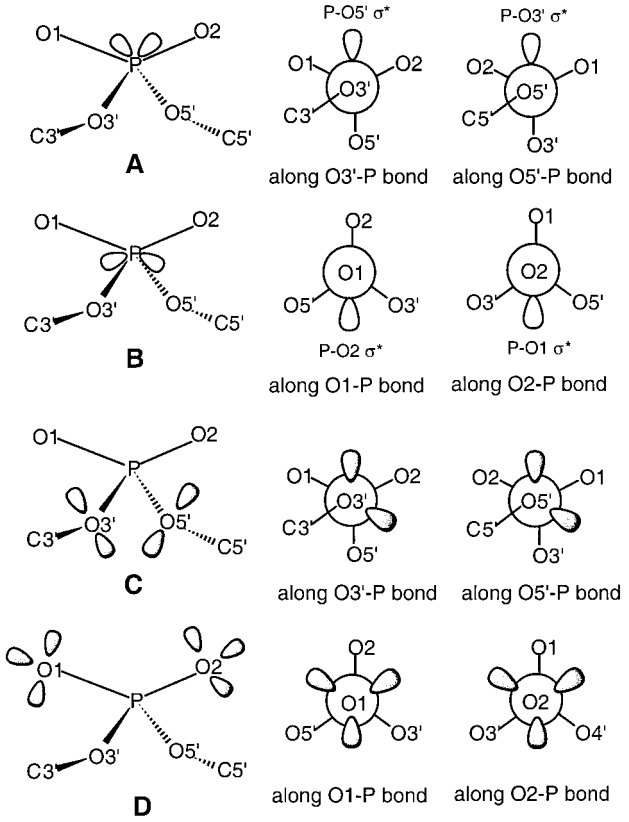

Figure 4. Selected antibonding orbitals and lone pairs involved in delocalizations that stabilize the phosphodiester moiety along with Newman projection diagrams. The phosphoramidate moiety differs only through the presence of a single lone pair on the N3′ atom. (A) $P-O_{ester}$ antibonding orbitals and (B) $P-O_{anionic}$ antibonding orbitals [all four antibonding orbitals are in the same orientation for all geometries studied]; (C) O_{ester} lone pairs for the *gg* geometry; and (D) $O_{anionic}$ lone pairs for the *gg* geometry. Note that the third lone pair on the anionic oxygens shown here is not described in the delocalization energy analysis in Figures 6 and 7 since the delocalization contribution of this lone pair to antibonding orbitals is small due to its partial participation in a π bond to the phosphorus atom. Only one lobe of each antibonding orbital is shown for the sake of simplicity.

NBO analysis[20] allows for specific lone pair to antibonding orbital delocalizations to be quantitated from which a detailed picture of their contributions to the energetics of different conformations can be obtained. The antibonding orbitals around the phosphorus atom can be classified as (1) antibonding orbitals for the $P-O_{ester}$ or P−N3′ bonds (Figure 4A, N3′ is not shown explicitly) and (2) antibonding orbitals for the $P-O_{anionic}$ bonds (Figure 4B). Correspondingly, the lone pairs located in the phosphodiester and phosphoramidate moieties can be classified into two types: (1) the ester position lone pairs located on the O3′, O5′, or N3′ (not shown) atoms (Figure 4C) and (2) the anionic position lone pairs located on the O1 or O2 atoms (Figure 4D). This list is selective in that it contains only the antibonding orbitals for the P−O bonds in this moiety. According to the conventional hypothesis, only the delocalizations of the O_{ester} (Figure 4C) or N lone pairs to the $P-O_{ester}$ (Figure 4A) or P−N antibonding orbitals contribute to the conformational energetics. In our hypothesis, every lone pair shown in Figure 4 can delocalize to each antibonding orbital shown, including the $O_{anionic}$ lone pairs and the $P-O_{anionic}$ orbitals, with all possible delocalizations contributing to the conformational energetics. Moveover, other delocalizations into antibonding orbitals not shown in Figure 4 (e.g. for C−H bonds) can occur, as discussed below.

The extent of delocalization and the corresponding stabilizing delocalization energy should be affected greatly by the spatial proximity between the lone pair donating the electrons and the antibonding orbital accepting them. Therefore, when the donor lone pair and acceptor antibonding orbital are close to each other the delocalization energy is expected to be large; when they are separated, this energy is expected to decrease dramatically. Only the lone pairs on the O_{ester} atoms move as a result of $P-O_{ester}$ bond rotation. The natural question to ask then is why consider the $O_{anionic}$ lone pairs? To answer this question, it is necessary to consider the possibility that each lone pair is being delocalized to different extents into different antibonding orbitals. An example is shown in Figure 5 involving delocalization the N3′ lone pair of phosphoramidate into the $O5'_{ester}$, $O1_{anionic}$, and $O2_{anionic}$ antibonding orbitals.

Quantitation of all possible delocalizations associated with the orbitals and lone pairs shown in Figure 4 are presented in Figures 6 and 7. The height of the bars in Figures 6 and 7 represents the extent of delocalization of a specific lone pair into a specific antibonding orbital in terms of the delocalization energy (in kcal/mol). As is evident, significant delocalizations are present for all the lone pairs. Thus, energy contributions of the delocalizations for the anionic oxygens as well as the ester oxygen or nitrogen lone pairs in the phosphodiester (**1**) and phosphoramidate (**2**) moieties are significant.

The first general observation that can be made is that each lone pair can delocalize to each antibonding orbital, as shown by finite delocalization energies for every possible delocalization when the data for all the geometries are considered together. For example, the O3′, 1 lone pair (Figure 6A) delocalizes to the P−O5′, P−O1, and P−O2 antibonding orbitals when the *gg*, *gt*, and *tt* geometries are considered together. The only delocalizations that do not occur mostly are "self-delocaliza-

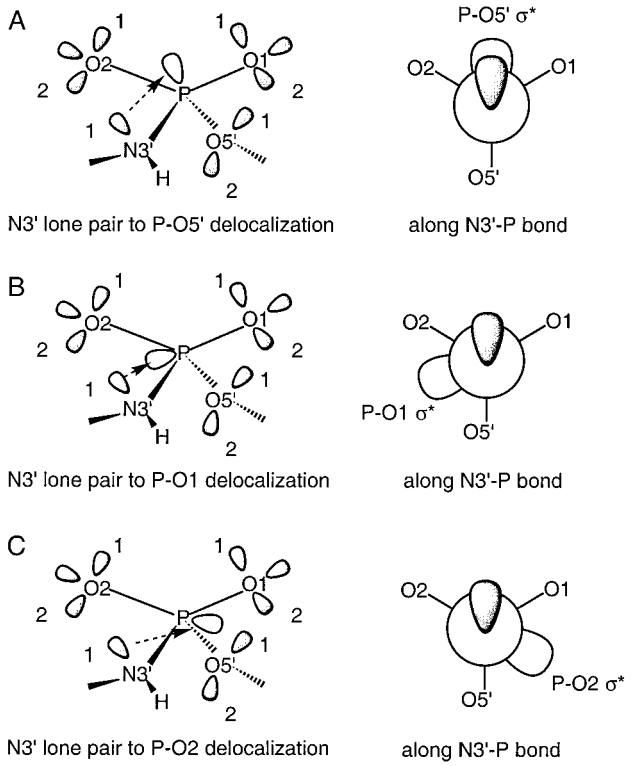

Figure 5. Pictorial depiction of three possible delocalizations of the N3′ lone pair (denoted by arrows) occurring in the N3′-phosphoramidate moiety along with the corresponding Newman projections diagrams. Delocalizations into the (A) P−O5′, (B) P−O1, and (C) P−O2 antibonding orbitals are depicted.

tions" of atomic lone pairs into antibonding orbitals for bonds containing the same donor atom. For example, delocalization of an O3′ lone pair into a P−O3′ antibonding orbital is not observed (Figure 6A). An exception is the self-delocalization of the O2, 2 lone pair to the P−O2 antibonding orbital for the *tt* geometry of **2** (Figure 7H).

The second general observation is that each antibonding orbital can accommodate delocalizations from multiple lone pairs. For example, for the *gg* geometry of **1**, all four $O_{anionic}$ lone pairs listed show delocalization into the P−O5′ antibonding orbital (Figure 7). This observation is critical to understanding why, even when the $O_{anionic}$ lone pairs do not change positions, their delocalizations to the antibonding orbitals change. This is due to the decrease in O_{ester} lone pair contributions to a specific antibonding orbital being compensated by an increase in delocalization to that antibonding orbital from the other lone pairs in its proximity. For example, in going from the *gt* geometry to the *tt* geometry of **1**, the decrease in the delocalization from the O5′, 2 lone pair to the P−O3′ antibonding orbital (Figure 6D, solid bar) is partially compensated by increases in the O5′, 1 (Figure 6C, solid bar), the O1, 2 (Figure 7B, solid bar), and the O2, 2 (Figure 7D, solid bar) lone pair delocalizations to the same orbital. In other words, adjustments occur in each delocalization upon a change in conformation. These adjustments originate due to the change in position of the O_{ester} and N3′ lone pairs but are clearly not limited to delocalizations involving just these lone pairs.

For both compounds, there is an asymmetry in the participation of the two lone pairs on the ester oxygens (O3′ or O5′) in the delocalization into P−O or P−N antibonding orbitals. One of the lone pairs (arbitrarily named the second lone pair, Figure 6B,D,G) shows greater delocalization to the P−O or P−N antibonding orbitals (solid or empty bars) than the other

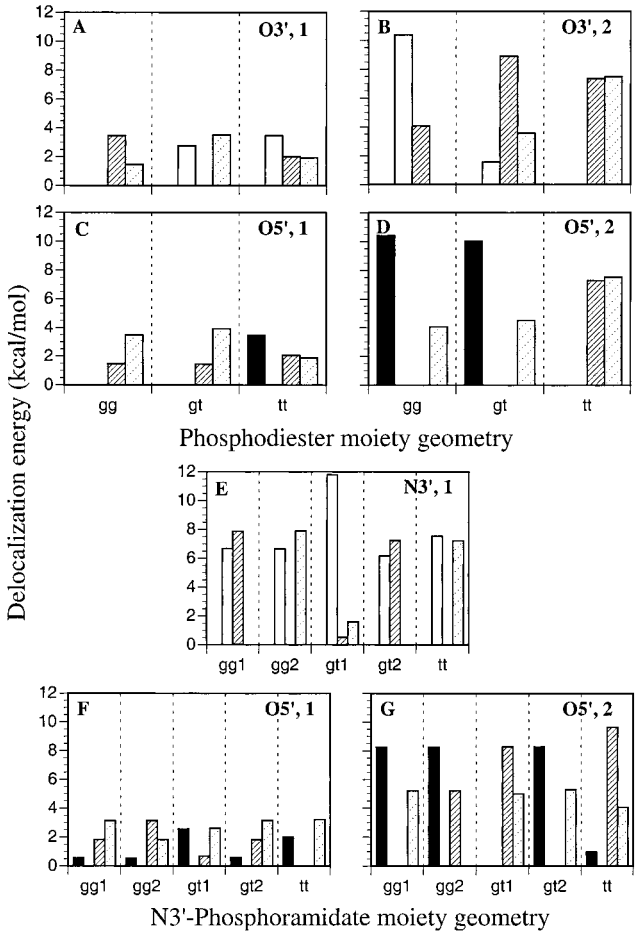

Figure 6. NBO electronic delocalization energies of each ester position lone pair to various P−X antibonding orbitals for the phosphodiester (**1**) and phosphoramidate (**2**) moieties. Each panel corresponds to delocalization of a single lone pair into different P−X antibonding orbitals: A, B, C, and D panels correspond to **1**; E, F, and G panels correspond to **2**; A, O3′ lone pair 1; B, O3′ lone pair 2; C, O5′ lone pair 1; D, O5′ lone pair 2; E, N3′ lone pair 1; F, O5′ lone pair 1; G, O5′ lone pair 2. Solid black bars show the P−O3′ antibonding orbital in **1** or **the** P−N3′ antibonding orbital in **2**; open bars show the P−O5′ antibonding orbital; slashed bars show the P−O1 antibonding orbital; and dotted slashed bars show the P−O2 antibonding orbital. Different geometries are separated by vertical dashed lines.

(compare parts A and B, C and D, and F and G in Figure 6). This second lone pair (Figure 6B,D, G), however, delocalizes to the corresponding P−N3′ or P−O3′ antibonding orbital (solid black bars) only when the N3′−P−O_{ester}−C or the O3′−P−O_{ester}−C dihedral is in the gauche orientation. This is consistent with the fact that when these dihedrals go to the trans orientation, the spatial proximity of this second lone pair to the P−N3′ or P−O3′ antibonding orbital decreases. Similar changes are observed for the first lone pair on each ester oxygen (Figures 6A,C,F). This shows that the spatial proximity rule applies irrespective of the magnitude of the delocalization contributions.

Energies associated with the anionic lone pair delocalizations are much stronger than those associated with the ester lone pair delocalizations as evidenced by the different scales of the delocalization energies between Figure 6 and Figure 7. This, in itself, provides a good reason for not ignoring these contributions. Moreover, it may be speculated that hydrogen bonding with solvent molecules, ions, or protein residues is likely to affect the magnitudes of each of these delocalizations such that a change in the conformational properties of the phosphodiester or phosphoramidate backbone may be observed. Such a

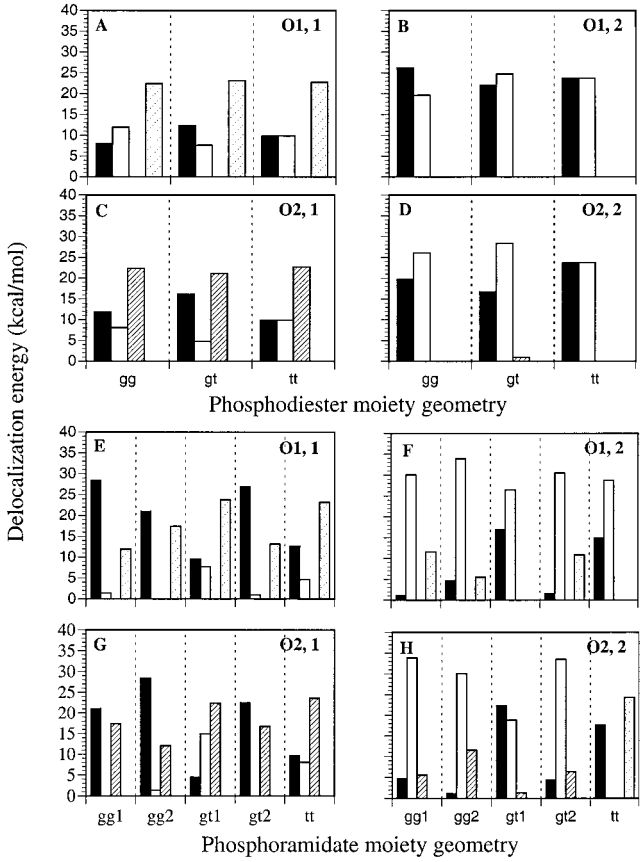

Figure 7. NBO electronic delocalization energies of each anionic position lone pair to various P−X antibonding orbitals for phosphoramidate (**2**) and phosphodiester (**1**) moieties. Each panel corresponds to delocalization of a single lone pair into different P−X antibonding orbitals: A, B, C, and D panels correspond to **1**; E, F, G, and H panels correspond to **2**; A, O1 lone pair 1; B, O1 lone pair 2; C, O2 lone pair 1; D, O2 lone pair 2; E, O1 lone pair 1; F, O1 lone pair 2; G, O2 lone pair 1; H, O2 lone pair 2. Solid black bars show the P−O3′ antibonding orbital in **1** or the P−N3′ antibonding orbital in **2**; open bars show the P−O5′ antibonding orbital; slashed bars show the P−O1 antibonding orbital; dotted slashed bars show the P−O2 antibonding orbital. Different geometries areseparated by vertical dashed lines.

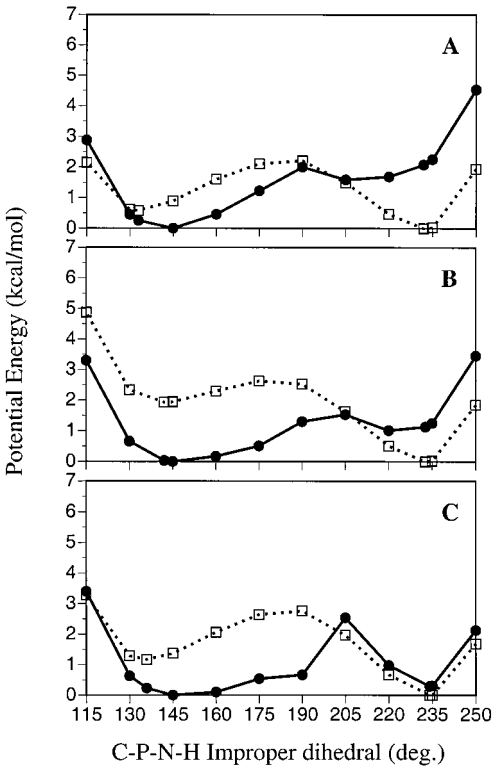

Figure 8. Potential energy inversion surfaces of the N3′−H moiety for compounds (A) **2**, (B) **3**, C2′-endo sugar pucker, and (C) **3**, C3′-endo sugar pucker. Gas-phase surfaces are indicated by a dotted line and a □, and the aqueous phase surfaces are indicated by a bold line and a ●. **2** is in the *gg*2 geometry corresponding to the experimentally observed geometry (see Table 1 and Figure 3).

phenomena may explain the previously reported results[30] as well as those in Table 1 where the relative energies of the *gg*, *gt*, and *tt* conformers change upon going from the gas phase to the aqueous phase.

This brings us back to the question that the original hypothesis sought to answer: why is the *gg* orientation favored over the *gt* and *tt* orientations? It is clear from our results that it is not only the O_{ester} or N3′ lone pair delocalizations that are responsible for the relative energy differences in **1** and **2**. The $O_{anionic}$ lone pair delocalizations also play an important role as do the P−$O_{anionic}$ antibonding orbitals. In addition to those listed above, the QM calculations also take into account various other possible delocalizations, such as the delocalization of O_{ester} lone pairs into C−H antibonding orbitals. The omission of these other acceptor orbitals in the present study is to simplify the picture of the stereoelectronic effects and does not reflect on their importance in terms of the stabilizing delocalization energy. In some cases (not shown), these contributions can be as significant as some of the O_{ester} lone pair to P−O antibonding orbitals listed here. The third lone pair on the anionic oxygens is another contributor not included in the analysis since delocalization contributions of this lone pair to antibonding orbitals are small. This may be due to its partial participation in a π bond to the phosphorus atom. It has been noted before that the full anomeric effect can only be explained on the basis of a combination of steric, electrostatic, and stereoelectronic effects.[37] On the basis of these considerations and the various delocalization contributions presented in Figures 6 and 7, it is proposed that the relative stability of the different conformers of **1** and **2** is due to a complex mixture of electronic delocalizations combined with other factors. This is in contrast with the previous view that one or two delocalizations associated with the ester O or N dominate the conformational energetics. Further support for this hypothesis is obtained from the energetics associated with inversion of the N3−H group and changes in partial atomic charges upon change in geometry (see below).

2. N3′−H Orientation in N3′-Phosphoramidate. It is known that lone pairs on electronegative atoms play an important role in controlling barrier heights to inversion.[38] The orientation of the N3′−H moiety has been postulated to be determined by delocalization of the N3′ lone pair into the P−O5′ antibonding orbital[9] (Figure 2). Figure 8A−C shows the inversion energy surfaces of the N3′−H moiety in **2** and **3** in the gas phase and aqueous phase for the *gg* conformer. There are two minima in **2** corresponding to the two possible orientations of the hydrogen on the gas-phase inversion surface (Figure 8A). The potential energy difference between the two minima is 0.6 kcal/mol and the energy barrier is 2.2 kcal/mol. The small relative energy difference between the minima and the low barrier height indicates that the change in orientation of the hydrogen is energetically feasible in the gas phase. To investigate the effect

(37) Tvaroska, I.; Bleha, T. *Adv. Carbohydr. Chem. Biochem.* **1989**, *47*, 45.

(38) Pophristic, V.; Goodman, L.; Guchhait, N. *J. Phys. Chem. A* **1997**, *101*, 4290−4297.

Table 4. Natural Population Analysis Charges for **1** and **2** in the Gas Phase Calculated at the MP2/6-31+G(d) Level of Theory

geometry of **1**	atoms assigned charges				
	P	O3′	O5′	O1	O2
gg	2.786	−0.953	−0.953	−1.262	−1.262
gt	2.782	−0.945	−0.952	−1.278	−1.255
tt	2.770	−0.935	−0.935	−1.270	−1.270

geometry of **2**	atoms assigned charges					
	P	N3′	O5′	O1	O2	HN3′
gg1	2.721	−1.133	−0.953	−1.267	−1.279	0.403
gg2	2.721	−1.133	−0.953	−1.279	−1.267	0.403
gt1	2.721	−1.125	−0.963	−1.270	−1.276	0.404
gt2	2.720	−1.130	−0.949	−1.267	−1.281	0.399
tt	2.712	−1.119	−0.944	−1.275	−1.283	0.400

of aqueous solvation on the N3′−H inversion surface, single-point calculations using the IPCM model on the optimized structures from the gas-phase surfaces were performed. The aqueous phase surface for **2** (Figure 8A) shows that solvation alters the inversion energy surface of the N3′−H moiety. The orientation corresponding to a C−P−N−H dihedral of ∼145° becomes the lowest energy conformation, with the second energy minimum at ∼205° having a relative energy of 1.6 kcal/mol, and the energetic barrier between the two minima being 2.0 kcal/mol. This lowest energy orientation of the N3′ hydrogen is consistent with the experimental predictions for the conformation of the N3′−H moiety in phosphoramidate DNA.[9,11]

The previous hypothesis of the anomeric effect in the phosphoramidate backbone cannot explain energetics associated with inversion of the N3′ hydrogen. This is due to such an inversion leading to loss of the N3′ ester lone pair to O5′ ester antibonding orbital delocalization, as shown in Figure 1B,C. An explanation for the small energy difference between the two minima for the N3′−H moiety (0.6 kcal/mol, Figure 8A) can be formulated only on the basis of our modified hypothesis of electronic delocalizations in the N3′-phosphoramidate moiety. If the P−O5′ antibonding orbital was the only available antibonding orbital to which the N3′ lone pair can delocalize, a large energetic difference for the two inversion states would be expected. However, the P−$O_{anionic}$ antibonding orbitals provide alternative delocalization orbitals for the N3′ lone pair (Figure 5, Figure 6E, *gg1* vs *gg2*, *gt1* vs *gt2*, slashed and dotted-slashed bars, respectively). Thus, when the orientation of the N3′ lone pair changes due to inversion of the N3−H group, compensatory stabilization is achieved by increased delocalization into P−O1 and P−O2 antibonding orbitals and a large energetic penalty is avoided.

3. Changes in Partial Atomic Charge. In addition to the geometric and NBO analysis, evidence for stereoelectronic delocalizations can be obtained from changes in partial atomic charge for the different conformations. For example, when electronic delocalizations to the antibonding orbitals around the phosphorus atom increase, a decrease in its partial positive charge is expected, along with corresponding decreases in the partial negative charges of the lone pair-containing donor atoms. Natural Population Analysis charges for different geometries of **1** and **2** in the gas phase are shown in Table 4.

For **1** charge distributions vary depending on the geometry (Table 4). These variations occur in all atoms supporting the suggestion that changes in electronic delocalizations involve all atoms. The variations are ∼0.018 units or less in the O atoms. For example, the atomic charges on O3′ and O5′ both change from −0.953 to −0.935 in going from the *gg* to the *tt* geometry. The decrease in positive charge on the P atom for the same geometry change is, however, only 0.016 units, which is much smaller than the overall decrease expected just based on the O_{ester} atom partial charge change. This is because the decrease in negative charge on the O_{ester} atoms is partially compensated by an increase in the negative charge in the $O_{anionic}$ atoms (∼0.008 units), again demonstrating the involvement of the $O_{anionic}$ atoms in the stereoelectronic balance. For **2** charge distribution changes are also seen in response to the different conformations (Table 4). These variations again occur in all atoms. The variations are ∼0.019 units or less in the N3′ and O5′ atoms while they are ∼0.016 units or less in the $O_{anionic}$ atoms. For example, the atomic charge on the N3′ atom changes from −1.133 to −1.125 in going from the *gg2* to the *gt2* geometry. The charge on the O2 atom changes in the opposite direction, going from −1.267 to −1.276. There is no change in the partial positive charge on the P atom for the same geometry change. The general observations from this analysis are that partial atomic charges change upon geometric alterations presumably due to the change in electronic delocalizations, and the extent of change in charge is specific for the type of atom and its location in the moiety. These observations are consistent with our hypothesis of a complex balance of stereoelectronic effects responding to the changes in geometry.

4. Sugar Pucker in N3′-Phosphoramidate. The presence of a sugar moiety is postulated to affect the inversion of the hydrogen due to the gauche effect.[14] Inversion surfaces for **3**, which includes a deoxyribose sugar attached to the phosphoramidate moiety, were therefore determined. To assess the effect of the conformation of the furanose sugar on the inversion surface for the N3′−H moiety, the sugar conformation was fixed in either the C2′-endo or C3′-endo conformations, representative of B-DNA and A-DNA, respectively (Figure 8, parts B and C, respectively). Comparison of these inversion surfaces for the two sugar puckers shows that the potential energy difference between the two minima is 1.9 kcal/mol for the C2′-endo sugar pucker (Figure 8B) and 1.2 kcal/mol for the C3′-endo sugar pucker in the gas phase (Figure 8C). Thus, the C3′-endo sugar pucker results in a decreased relative energy difference between the two inversion minima. For **3** with the C2′-endo sugar conformation (Figure 8B), inclusion of aqueous solvation results in a shift of the minimum from a C−P−N−H improper dihedral value of 233° to 145°. The energy difference between the two orientations also changes from 1.9 kcal/mol in the gas phase to 1.0 kcal/mol. With the C3′-endo sugar conformation (Figure 8C), inclusion of aqueous solvation also results in a change of the minimum energy conformation from 234° to 145° and the energy difference between the two minima is decreased from 1.2 kcal/mol to 0.3 kcal/mol. The barrier height between the two minima decreases slightly from 2.8 kcal/mol in the gas phase to 2.5 kcal/mol in the aqueous phase. These results suggest that the sugar conformation has subtle effects on the orientational freedom of the N3′−H moiety which vary upon going from the gas phase to the aqueous phase environment.

A remarkable effect of the aqueous environment on the energetics of **3** is demonstrated by comparing the above inversion surfaces for the C2′-endo and C3′-endo conformations against the global minimum energy state for both sugar conformations (Figure 9A,B). In the gas phase (Figure 9A), the two energy surfaces are different, especially near the minimum energy conformation of ∼230°, with the C2′-endo conformation having the overall lower energy surface. This suggests that the electronegativity of the 3′-substituent with the sugar conformation does not behave as expected[14] in the gas phase. However, in the aqueous phase a crucial difference is observed between

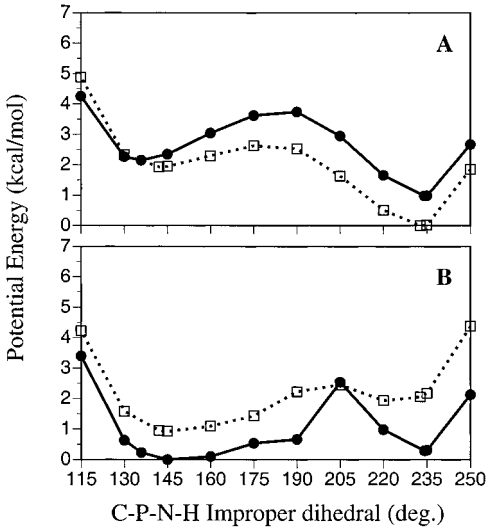

Figure 9. Potential energy inversion surfaces of the N3′−H moiety for compound **3** in the (A) gas phase and (B) aqueous phase. C2′-endo surfaces are indicated by a dotted line and a □; C3′-endo surfaces are indicated by a bold line and a ●.

the two sugar conformation inversion surfaces (Figure 9B). The inversion surface for the C2′-endo conformation is shifted to higher energy values as compared to the C3′-endo conformation surface. In fact, the two surfaces show similar energies only for the transition state dihedral (205°) of the C3′-endo surface, where the difference is less than 0.1 kcal/mol favoring the C2′-endo conformation. This overall higher energy for the C2′-endo conformation in the aqueous phase clearly suggests that it is mainly the aqueous environment that causes the stabilization of the C3′-endo conformation of the sugar in N3′-phosphoramidate.

Conclusions

On the basis of QM calculations, the anomeric effect in the phosphodiester moiety of DNA is suggested to be more complicated than previously hypothesized.[5] Geometry changes and NBO analysis demonstrate that, in addition to delocalizations involving O_{ester} or N3′ lone pairs and $P-O_{ester}$ antibonding orbitals, delocalizations involving $O_{anionic}$ lone pairs and $P-O_{anionic}$ antibonding orbitals also occur. A complex balance between all these delocalizations is maintained in response to conformational changes in these moieties. Solvation changes may influence the nature of these delocalizations, which may be a prominent factor in governing the changes in conformational properties of these moieties seen to occur upon solvation.[30,31]

Energy differences associated with inversion of the N3′−H moiety in N3′-phosphoramidate are seen to be quite small. It is postulated therefore that the N3′−H moiety is flexible both in the gas phase and in aqueous solution. This flexibility is inconsistent with the previous hypothesis of the anomeric effect in the N3′-phosphoramidate backbone[9] since the one stabilizing interaction postulated in this hypothesis is lost upon N3′−H inversion. Our modified hypothesis shows alternative delocalization possibilities for the N3′ lone pair to the $P-O_{anionic}$ antibonding orbitals, thereby preventing significant energetic penalties upon inversion.

The importance of solvation effects has been noted in previous theoretical studies of duplex stability of the A-form N3′-phosphoramidate structure.[39] In the present study, a previously unreported and profound effect in the stabilization of the C3′-endo conformation is observed due to the presence of an aqueous solvation environment. Changes in solvation associated with the N3′−H substitution observed experimentally, like the increased hydration of N3′-phosphoramidate backbone,[9,11] therefore may play a crucial role in determining its structural properties.

Acknowledgment. This work has been supported by NIH grant GM-51501. We thank the Pittsburgh Supercomputing Center, the DOD ASC Major Shared Resource Computing, and the National Partnership for Advanced Computational Infrastructure (NPACI) for providing computational resources. We thank Dr. Daniel Barsky for helpful discussions regarding the phosphoramidate results.

Supporting Information Available: *XYZ* files of all the structures in Figure 3, including the MP2/6-31+G* energies, are presented along with the minimum energy structures for **3** from Figure 8B,C (PDF). This material is available free of charge via the Internet at http://pubs.acs.org.

JA010295W

(39) Barsky, D.; Colvin, M. E.; Zon, G.; Gryaznov, S. M. *Nucleic Acids Res.* **1997**, *25*, 830−835.